J. Braz. Chem. Soc., Vol. 20, No. 9, 1632-1637, 2009.
Printed in Brazil - ©2009 Sociedade Brasileira de Química
0103 - 5053 $6.00+0.00

Article

Influences of Heat Treatment on the Structure and Electrochemical Properties of $Mg_{0.9}Ti_{0.1}Ni$ Hydrogen Storage Alloys

HongXia Huang,[a,b] KeLong Huang,[,a] SuQin Liu,[a] DongYang Chen[a] and ShuXin Zhuang[a]*

[a]*College of Chemistry and Chemical Engineering, Central South University, Changsha 410083, PR China*

[b]*The Department of Material and Chemistry of Guilin University of Technology, Guilin 541004, PR China*

Neste trabalho, os efeitos do tratamento térmico nas estruturas e propriedades eletroquímicas de ligas para armazenamento de hidrogênio $Mg_{0.9}Ti_{0.1}Ni$ foram investigadas em detalhe. As análises por difração de raios-X (XRD) e microscopia eletrônica (SEM) mostraram que as amostras exibiram predominantemente uma estrutura amorfa. Estudos eletroquímicos revelaram que o tratamento térmico pode melhorar a capacidade máxima de descarga e ciclabilidade dos eletrodos desta liga. O valor de C_{max} à liga $Mg_{0.9}Ti_{0.1}Ni$ preparada por moagem, foi de apenas 229,9 mAh g^{-1}; entretanto, o valor atingiu 331,9 mAh g^{-1} após o tratamento térmico a 873K por 8 h seguido de moagem. A voltametria cíclica, espectroscopia de impedância eletroquímica e polarização potenciodinâmica indicaram que o tratamento térmico não só aumentou a capacidade de descarga, mas também melhorou a cinética de carga/descarga da liga $Mg_{0.9}Ti_{0.1}Ni$.

In the present study, the effects of heat treatment on the structures and electrochemical properties of $Mg_{0.9}Ti_{0.1}Ni$ hydrogen storage alloys have been investigated in detail. X-ray diffraction (XRD) and scanning electron microscopy (SEM) analyses showed that the samples exhibited a predominantly amorphous structure. Electrochemical investigations revealed that heat treatment can improve the maximum discharge capacity and cyclic stability of the alloy electrodes. For $Mg_{0.9}Ti_{0.1}Ni$ alloy prepare by ball milling, the value of C_{max} was only 229.9 mAh g^{-1}, however, the value reached 331.9 mAh g^{-1} after heat treatment at 873K for 8 h and then milling. The cycle voltammetry, electrochemical impedance spectroscopy and potentiodynamic polarization indicated that heat treatment not only increased the discharge capacity but also improved the charge/discharge kinetics of $Mg_{0.9}Ti_{0.1}Ni$ alloy.

Keywords: hydrogen absorbing materials, amorphous materials, heat treatment, electrochemical properties

Introduction

Recently, the MgNi-based hydrogen storage alloys has been considered as one of the most attractive candidates for metal hydride electrode materials of the nickel metal hydride (Ni/MH) rechargeable batteries because of their high hydrogen storage density, low specific gravity, low cost, abundant resource and environmental friendly. The theoretical capacity of MgNi is 1080 mAh g^{-1} and the initial discharge of amorphous MgNi alloy is 500 mAh g^{-1}.[1] Despite their merits, practical application of this kind of alloys has been hampered by the deterioration of discharge capacity in alkaline solution and the high temperature needed for their absorption and desoption. For this purpose, worldwide researchers have carried out a lot of investigations to improve the cyclic stability and kinetics properties of these alloys, including (*i*) substitution of alloy elements;[2,3] (*ii*) surface treatment;[4] (*iii*) elaboration of alloy composite. Since Mg is the corrosion sensitive element in MgNi, it appears that partial substitution of Mg is an effective method for improving the cycle life of the MgNi based electrodes. Several works have shown that Ti as partial substitute for Mg in MgNi and Mg_2Ni alloys is an effective methods in improving the electrode cycle life.[5-10] This is associated with the formation of a more compact and more protective titanium oxides on the alloy surface which limits further oxidation of Mg and induces a Ni enriched layer on the alloy surface.[11] Yuan *et al.*[12] reported that the discharge capacity of the $Mg_{0.9}Ti_{0.1}Ni$ alloy milled for 120 h reached 356.85 mAh g^{-1}. In addition,

*e-mail: huangkelong@yahoo.com.cn

the preparation technology is also very important for improving the overall performance of alloys. Sakai *et al.*[13] reported that heat treatment could decrease the crystal defects and increase alloy composition homogenization, and consequently enhance the discharge capacity and cyclic stability of hydrogen storage alloys. Zhang *et al.*[14] investigated the effect of annealing treatment on structure and electrochemical properties of $La_{0.67}Mg_{0.33}Ni_{2.5}Co_{0.5}$ alloy electrodes and achieved better maximal discharge capacity and the cyclic stability. Zhao *et al.*[15] discussed the effects of different heat treatment methods on $La_{0.67}Mg_{0.33}Ni_{2.5}Co_{0.5}$ alloy and reported that the alloys obtained by magnetic-heat treatment exhibited the best discharge capacity with better activation property and larger capacity retention.

This paper focus on the investigation of the effect of heat treatment on the structures and electrochemical properties of $Mg_{0.9}Ti_{0.1}Ni$ hydrogen storage alloys, it is found that heat treatment could favor the discharge capacity and the cyclic stability.

Experimental

$Mg_{0.9}Ti_{0.1}Ni$ alloy sample was prepared by ball milling from magnesium, nickel power and titanium power, respectively. The mixture was milled for 80 h at a speed of 225 rpm in an argon filled stainless steel vessel, employing a ball to powder weight ratio of 20:1. The purity of all the starting elemental metals was not lower than 99.0%. The alloy was represented as as-milled.

In comparison, a typical experimental procedure for heat treatment+milling sample was as follows: The metal powers for stoichiometric $Mg_{0.9}Ti_{0.1}Ni$ were first ultrasonic in N,N-dimethyl formamide for 30 min, and then treated at 873 K for 5 h under an argon atmosphere after centrifugation, the latter detailed process was the same as the method for as-milled sample. The alloy was represented as heat treatment+milling.

The structures and surface morphologies of the alloys were collected by powder X-ray diffraction using Japan D/max 2550 VB+18 kV diffractometer using CuK_{α} radiation (λ = 1.54178 Å) and Scanning electron microscopy (SEM, JSM-6360 LV).

Electrodes for tests were prepared as follows: 0.3 g of the mixture of as-prepared powder and carbonyl nickel power (mass ratio 1:2) were cold pressed into a round pellet of 10 mm in diameter under a pressure of 10 MPa and then pressed at 20 MPa between two pieces of foam nickel.

The test electrode pellets were immersed in 6 mol L^{-1} KOH solution for 2 h in order to make it wet fully before the electrochemical measurement. Charge/discharge tests employed a half-cell consisting of working electrode (as-prepared electrode), sintered $NiOOH/Ni(OH)_2$ as counter electrode, and 6 mol L^{-1} KOH solution as electrolyte. The discharge capacity, activation ability and cyclic stability were performed using an automatic Land battery test instrument. The test sequence was that charged at 100 mA g^{-1} for 6 h, discharged at 25 mA g^{-1} to the cut-off voltage of 0.8 V, rest for 10 min between charge and discharge.

CHI 660B electrochemical workstation was used for cycle voltammetry (CV) (scan rate: 1 mV s^{-1}, −1.2 V to −0.2 V *vs.* HgO/Hg), potentiodynamic polarization (scan rate: 1 mV s^{-1}, −1.0 V to −0.2 V *vs.* HgO/Hg), and electrochemical impedance spectroscopy (EIS) (open circuit potential, amplitude 5 mV, 1×10^3 Hz to 10^{-3} Hz) measurements. During CV, EIS and potentiodynamic polarization tests, HgO/Hg as reference electrode. In order to reduce the ohmic drop between the working electrode and the reference electrode, a Luggin capillary was located close to the hydride electrode. The environmental temperature of the experiments was kept at 30 °C.

Results and Discussions

Phase structures

Figure 1 presents the XRD patterns of the as-milled and heat treatment+milling $Mg_{0.9}Ti_{0.1}Ni$ hydrogen storage alloys. It can be seen that the two samples exhibited a predominantly amorphous structure. The position of the diffraction peak is around 43° and is not shifted by sintering treatment. With heat treatment, the relative intensity of diffractive peak is declined and the peak becomes broader, it means the abundance of amorphism of heat treatment+milling alloy is larger. In addition, the mean particle size of alloy powder becomes smaller and the internal stress increases, which is advantageous for the transformation from crystalloid to amorphous structure and improves the cycle capacity of heat treatment+milling, it is discussed further in section “Discharge capacities and cycle stability”.

Surface morphology

The morphologies of the $Mg_{0.9}Ti_{0.1}Ni$ hydrogen storage alloy are investigated by SEM as shown in Figure 2. The SEM images of as-milled alloy is shown in A, the particles varies from 1 to 4 μm in diameter, B is the SEM image of heat treatment+milling alloy, the bulk average particle size is between 1-3 μm in diameter. Compared to as-milled sample, it is obvious that particle size and the interspaces of heat treatment+milling alloy become smaller and less conglomerated than that of as-milled sample, and the heat

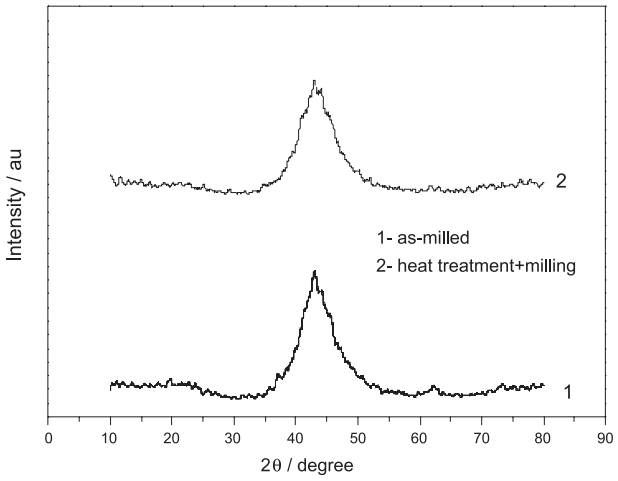

Figure 1. XRD patterns of as-milled and heat treatment + milling $Mg_{0.9}Ti_{0.1}Ni$ hydrogen storage alloys.

treatment is favorable to the homogeneity of composition, which may accelerate the electrochemical reaction of the hydrogen on the surface of the alloy particles due to the increase of specific surface area.

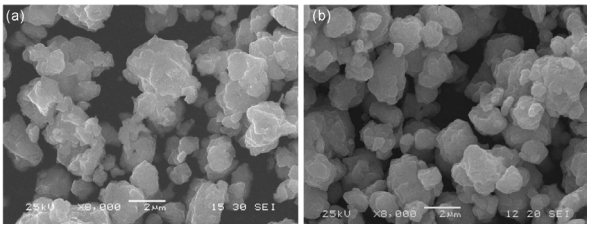

Figure 2. SEM images of as-milled and heat treatment+milling $Mg_{0.9}Ti_{0.1}Ni$ hydrogen storage alloys. (a) as-milled; (b) heat treatment+milling.

Discharge capacities and cycle stability

Figure 3 exhibits the curves of discharge capacities *vs.* cycle numbers of the as-milled and heat treatment+milling $Mg_{0.9}Ti_{0.1}Ni$ alloy electrodes. It can be seen that two alloy electrodes are fully activated within three cycles and the heat treatment+milling electrode exhibites the largest discharge capacity at the first cycle. This indicates that heat treatment has a positive effect on the activation property of the alloy electrodes. Table 1 presents the activation properties (N_a), maximum discharge capacity (C_{max}) and cycling stability (C_{20}/C_{max} and C_{30}/C_{max}) of the two $Mg_{0.9}Ti_{0.1}Ni$ alloy electrodes. As can be seen in Table 1, heat treatment can enhance the maximum discharge capacity of the alloy electrodes from 229.9 mAh g^{-1} to 331.9 mAh g^{-1}. The cycling stability C_{20}/C_{max} and C_{30}/C_{max} increased from 27.4% (as-milled) to 63.7% (heat treatment+milling) and from 17.2% (as-milled) to 59.4% (heat treatment+milling). Three reasons are responsible for the degradation of the discharge capacity of the MgNi-based hydrogen storage alloy electrodes, one of them is that the pulverization of the alloys during the repeated charging and discharging cycles, which produce unprotected fresh surface and consequently, resulting in the degradation of capacity of the alloy electrodes; the second is the oxidation and corrosion of the alloy components in strong alkaline solution to $Mg(OH)_2$, which cannot prevent the electrolyte from corroding the alloy further and baffles the diffusion of hydrogen atoms;[16] the last is the transformation from amorphous to crystalline of Mg_2NiH_4 and Ni. Mg_2NiH_4 is unable to desorb hydrogen at room temperature, so the alloy shows a very low electrochemical discharge capacity.[17-19] The improvement of the cyclic stability by heating in Ar at 873 K can be explained as follows. The heat treatment can refine the grains of alloy particles, improve the composition homogeneity and increase the amorphous phase, which will benefit to improvement of the cyclic stability of the alloy electrode. From Figure 1, the abundance of amorphism of heat treatment+milling alloy is larger than as-milled alloy. The diffusivity and solubility of hydrogen in amorphous phase is greater compared to crystalloid and the amorphous alloys offer not only outstanding anti-pulverization performance but also anti-corrosion capability,[20] so the increment of amorphous phase is responsible for above experimental results. Some researchers confirmed that heat treatment can increase the specific surface area due to the evaporation of magnesium and suppression the growth of magnesium hydroxide by the enriched Ni at the surface.[21]

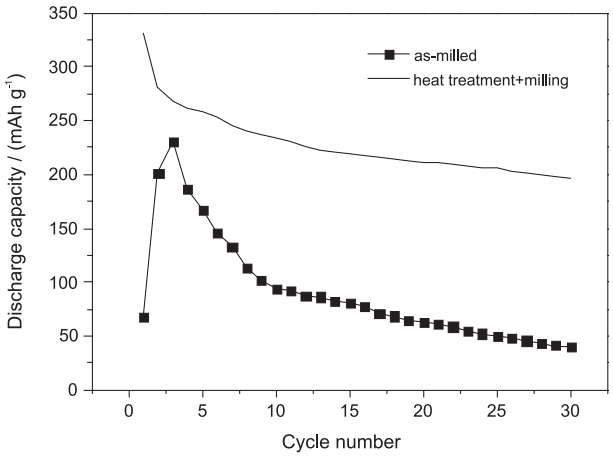

Figure 3. Curves of discharge capacities *vs.* cycle numbers for the as-milled and heat treatment+milling $Mg_{0.9}Ti_{0.1}Ni$ alloy electrodes.

Cyclic voltammetry (CV)

To investigate the phenomena described above, the electrochemical behavior of the two samples was measured. Figure 4 exhibits the CV curves of as-milled and heat

Table 1. The electrochemical characteristics of the as- milled and heat treatment+milling alloy electrodes

Alloys	Na	C_{max}/(mAh g^{-1})	C_{20}/(mAh g^{-1})	C_{20}/C_{max} (%)	C_{30}/(mAh g^{-1})	C_{30}/C_{max} (%)
as-milled	3	229.9	62.9	27.4	39.5	17.2
heat treatment +milling	1	331.9	211.4	63.7	197.1	59.4

Na: The cycle numbers needed to activate the electrodes.

treatment+milling alloys at a scanning rate of 1 mV s^{-1} at the potential interval of −1.2 to −0.2 V *vs.* HgO/Hg. The anodic peak at around −0.85 V to −0.7 V *vs.* HgO/Hg was attributed to the dehydrogenation according to the following equation.[22]

$$MH_n + nOH^- \rightarrow M + nH_2O + ne^-$$

The cathodic peak at around −1.0 to −1.1 V *vs.* HgO/Hg was attributed to the hydriding according to above equation at opposite side. The anodic (oxidation) peak current might be used for evaluating the kinetics of hydride electrode for dehydrogenation and the peak area reflected the discharge capacity.[23] As seen in Figure 5, the height and area of oxidation peak for heat treatment+milling alloy electrode is larger than that of as-milled electrode, which indicates that the absorption and desorption of hydrogen in the alloy are remarkably accelerated and the active sites on the surface are greatly incremented after heat the treatment, this result coincides with that obtained from the maximum discharge capacity.

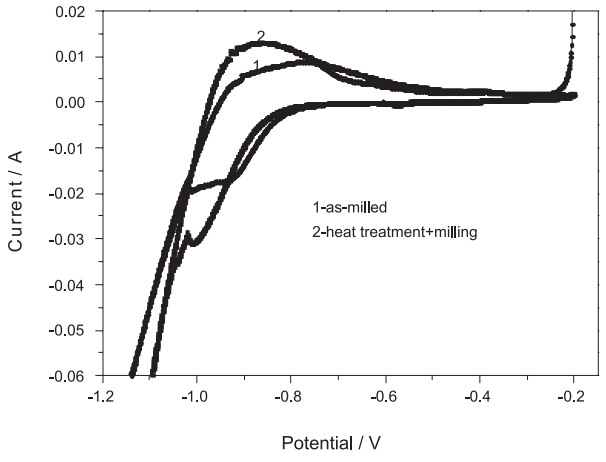

Figure 4. CV curves of as-milled and heat treatment+milling alloys at a scanning speed of 1 mV s^{-1}.

Potentiodynamic polarization

To estimate the kinetics of the absorption and desorption, polarization measurements were carried out on CS300 electrochemical testing system at a scanning rate of 1 mV s^{-1}. Figure 5 shows the potentiodynamic polarization curves for two electrodes, the results obtained through Tafel fitting are summarized in Table 2. The result reveals that the value of corrosion voltage (E_{corr}) of heat treatment+milling alloy is higher than as-milled alloy, and the value of corrosion current density (I_{corr}) is lower than that of as-milled alloy. It suggests that the anti-corrosion behavior of $Mg_{0.9}Ti_{0.1}Ni$ alloy is enhanced by the heat treatment. The main reason for this phenomenon is that the heat treatment favors the homogeneity of composition in alloy and the formation of amorphous phase. The increasing of amorphous phase could enhance not only the anti-pulverization performance but also the anti-corrosion capabilities of the hydrogen storage alloys.[19]

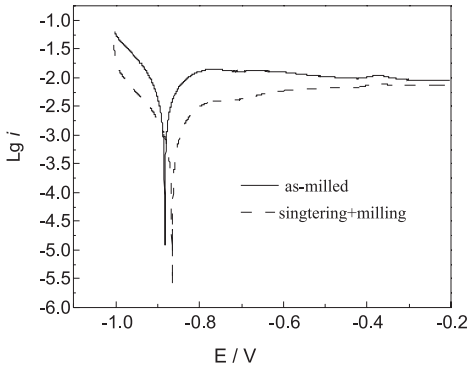

Figure 5. Potentiodynamic polarization curves of the as-milled and heat treatment+milling alloy electrodes.

Table 2. The corrosion voltage E_{corr} and corrosion current density I_{corr} of the as-milled and heat treatment+milling alloy electrodes

Alloys	E_{corr} / V	I_{corr} / (A cm^{-2})
as-milled	–0.78509	0.019869
heat treatment + milling	–0.76498	0.003058

Electrochemical impedance spectroscopy (EIS) analysis

Figure 6 shows the EIS plots for the as-milled and heat treatment+milling electrode alloys at 50% depth of discharge (DOD) and their proposed equivalent circuit. It can be seen that the spectra of the two samples compose of one semicircle and a linear Warburg part.[24] The semicircle in high frequency region is attributed to the charge transfer or electrochemical

reaction resistance (R_1), and the low frequency straight line is attributed to the diffusion resistance of hydrogen in the bulk alloy. On the basis of the circuit and by means of fitting with Z-VIEW program, the solution resistance and electrochemical reaction resistance values are obtained and listed in Table 3. It can be seen that the values of solution resistance (Rs) of heat treatment+milling alloy is larger than as-milled alloy, but the charge-transfer reaction resistance (R_1) of the alloys declines from 0.19454 Ω to 0.15823 Ω with heat treatment. It agrees well with the results from maximum discharge capacity, indicating that heat treatment could effectively improve the electro-catalytic activity of hydrogen storage alloys.

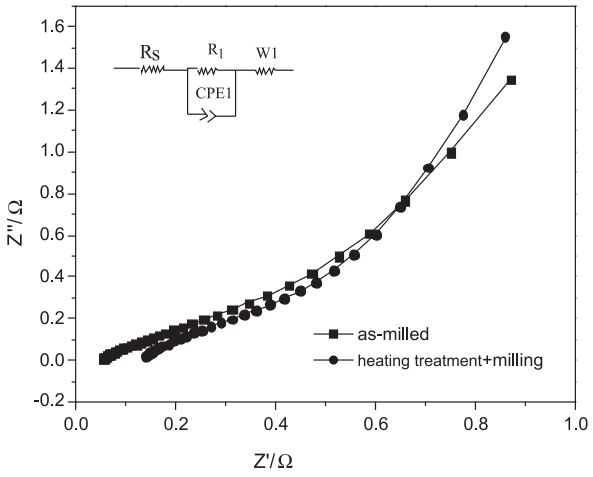

Figure 6. Electrochemical impedance spectra (EIS) of the as-milled and heat treatment+milling alloy electrodes.

Table 3. Calculated electrochemical parameters from electrochemical impedance spectra of the as-milled and heat treatment+milling alloy electrodes

Alloys	Rs / Ω	R_1 / Ω
as-milled	0.04964	0.19454
heat treatment+milling	0.13327	0.15823

Based on above discussion, heat treatment plays an important role in improving the electrochemical performances of $Mg_{0.9}Ti_{0.1}Ni$ hydrogen storage alloy. An excellent merit from a commercial point of view is that an extended period of activation is not necessary for heat treated alloys as it is the case for other alloys. Up to date, immense researches have been focused on the substitution of alloy elements. Nevertheless, surface modification technologies such as heat treatment are rarely investigated. Although the obtained result on electrochemical performance of alloy electrodes is not satisfactory for practical application, it has the potential of utility by improving the cycle performance of alloy electrode through combining further substitution of alloy elements and heat treatment technology. As an extension of this work, corresponding mechanism of heat treatment on the structure and electrochemical characteristics of hydrogen storage alloys will be further investigated.

Conclusions

In summary, $Mg_{0.9}Ti_{0.1}Ni$ hydrogen storage alloys were prepared by ball milling under argon atmosphere or treating at 873 K for 5 h and then ball milling. The phase structure and the main electrochemical properties of the two samples were investigated. Some conclusions can be summarized.

XRD diffraction analyses indicated that for both as-milled alloy and heat treatment+milling alloys exhibited a predominantly amorphous structure, and the composition became much homogeneous after heat treatment. The electrochemical studies revealed that the alloy electrodes can be easily activated to their maximum discharge capacity within three cycles. The maximum discharge capacity of the as-milled alloy electrodes was only 229.9 mAh g^{-1}. After treating at 873 K for 5 h, the discharge capacity and cyclic stability of the alloy electrode were improved, the initial discharge specific capacity of sample was 331.9 mAh g^{-1} and the discharge capacity retention (C_{30}/C_{max}) increases from 17.2% to 59.4% after 30 charge/discharge cycles, for which the better anti-corrosion and anti-oxidation capabilities was responsible. The potentiodynamic polarization result shown that the charge transfer resistance value (R_1) declined with heat treatment, which indicated that the kinetic property of $Mg_{0.9}Ti_{0.1}Ni$ alloy was improved.

Acknowledgments

This work was supported by the National Nature Science Foundation of China (50772133). The authors express their thanks to the colleagues of Institute of Functional Materials and Chemistry of Central South University for their experimental help.

References

1. Ruggeri, S.; Lenain, C.; Roué, L.; *Mater. Sci. Forum* **2001**, *11*, 63.
2. Wang, M. H.; Zhang, L. Z.; Zhang, Y.; Sun, L. X.; Tan, Z. C.; Xu, F.;Yuan, H. T.; Zhang, T.; *Int. J. Hydrogen Energy* **2006**, *31*, 775.
3. Goo, N. H. ; Lee, K. S.; *Int. J. Hydrogen Energy* **2002**, *27*, 433.
4. Souza, E. C.; Ticianelli, E. A.; *Quim. Nova* **2006**, *29*, 216.

5. Ruggeri, S. ; Rou´e, L. ; Huot, J. ; Schulz, R. ; Aymard, L. ; Tarascon, J.M. ; *J. Power Sources* **2002**, *112*, 547.
6. Chen, J.; Yao, P. ; Bradhurst, D. H. ; Dou, S. X. ; Liu, H. K.; *J. Alloys Compd*. **1999**, *293–295*, 675.
7. Yuan, H. T.; Yang, E. D.; Yang, H. B.; Liu, B.; Wang, L. B.; Cao, R.; Zhang, Y. S.; *J. Alloys Compd*. **1999**, *291*, 244.
8. Ye, H.; Lei, Y. Q.; Chen, L. S.; Zhang, H. V.; *J. Alloys Compd*. **2000**, *311*, 194.
9. Zhang, Y.; Liao, B.; Chen, L. X.; Lei, Y. Q.; Wang, Q. D.; *J. Alloys Compd*. **2001**, *327*, 195.
10. Zhang, Y.; Zhang, S. K.; Chen, L. X. ; Lei, Y. Q.; Wang, Q. D.; *Int. J. Hydrogen Energy* **2001**, *26*, 801.
11. Han, S. C.; Lee, P. S. ; Lee, J. Y. ; Züttel, A.; Schlapbach, L.; *J. Alloys Compd*. **2000**, *306*, 219.
12. Yuan, H. T.; Song, H. N.; Liu, Q. D.; *Chem. J. Chinese U*. **2003**, *24*, 584.
13. Sakai, T. ; Miyamura, H.; Kuriyama, N.; Ishikawa, H.; Uehara, I. Z.; *Phys. Chem.* **1994**, *183*, 333.
14. Zhang, F.; Luo, Y.; Chen, J.; Yan, R.; Kanga L.; Chen J.; *J. Power Sources* **2005**, *150*, 247.
15. Zhao, X. J. ; Li, Q. ; Chou, K. C. ; Liu, H. ; Lin, G. W.; *J. Alloys Compd.,* **2008**, doi: 10.1016/j.jallcom.2008.05.108.
16. Liu, W. H. ; Lei, Y. Q. ; Sun, D. L. ; Wu, J. ; Wang, Q. D.; *J. Power Sources* **1996**, *58*, 243.
17. Liu, W. H.; Wu, H. Q.; Lei, Y. Q.; Wang, Q. D.;Wu, J.; *J. Alloys Compd.* **1997**, *252*, 234.
18. Orimo, S.; Fujii, H.; *J. Alloys Compd.* **1996**, *232*, L16.
19. Zaluski, L.; Zaluska, A.; Ström-Olsen, J. O.; *J. Alloys Compd.* **1995**, *217*, 245.
20. Zhang, Y. H.; Wang, G. Q.; Dong, X. P.; Guo, S. H.; Wu, J. M.; Wang, X. L.; *J. Alloys Compd*. **2005**, *398*, 178.
21. Hatano, Y.; Tachikawa, T.; Mu, D.; Abe, T.; Watanabe, K.; Morozumi, S.; *J. Alloys Compd*. **2002**, *330-332*, 816.
22. Chen, Y.; *Catal. Today* **1998**, *44*, 3.
23. Liu, Y. F.; Pan, H. G.; Gao, M. X.; Li, R.; Lei, Y. Q.; *J. Alloys Compd*. **2004**, *376*, 304.
24. Liu, W. H.; Wu, H. Q.; Lei, Y. Q.; Wang, Q. D.; *J. Alloy Compd*. **2002**, *346*, 244.

Received: July 22, 2008
Web Release Date: September 11, 2009